

## Related content

# A High-Granularity Timing Detector for the Phase-II upgrade of the ATLAS calorimeter system: detector concept description and first beam test results

To cite this article: D. Lacour 2018 *JINST* **13** C02016

- [Development of Ultra-Fast Silicon Detectors for 4D tracking](#)  
A. Staiano, R. Arcidiacono, M. Boscardin et al.

- [Performance of the ATLAS Liquid Argon Calorimeter after three years of LHC operation and plans for a future upgrade](#)  
P Strizenec

- [Sensors for the CMS High Granularity Calorimeter](#)  
A.A. Maier

View the [article online](#) for updates and enhancements.

RECEIVED: December 19, 2017

ACCEPTED: January 30, 2018

PUBLISHED: February 13, 2018

CHEF2017 — CALORIMETRY FOR THE HIGH ENERGY FRONTIER  
2–6 OCTOBER 2017  
LYON, FRANCE

## A High-Granularity Timing Detector for the Phase-II upgrade of the ATLAS calorimeter system: detector concept description and first beam test results

---

**D. Lacour**

*Laboratoire de Physique Nucléaire et de Hautes Énergies LPNHE CNRS/IN2P3,  
4, place Jussieu 75005 Paris, France*

*E-mail:* [lacour@cern.ch](mailto:lacour@cern.ch)

**ABSTRACT:** The expected increase of the particle flux at the high luminosity phase of the LHC (HL-LHC) with instantaneous luminosities up to  $7.5 \cdot 10^{34} \text{ cm}^{-2}\text{s}^{-1}$  will have a severe impact on the ATLAS detector performance. The pile-up is expected to increase on average to 200 interactions per bunch crossing. The reconstruction performance for electrons, photons as well as jets and transverse missing energy will be severely degraded in the end-cap and forward region. A High Granularity Timing Detector (HGTD) is proposed in front of the liquid Argon end-cap and forward calorimeters for pile-up mitigation. This device should cover the pseudo-rapidity range of 2.4 to about 4.0. Low Gain Avalanche Detectors (LGAD) technology has been chosen as it provides an internal gain good enough to reach large signal over noise ratio needed for excellent time resolution. The requirements and overall specifications of the High Granular Timing Detector at the HL-LHC will be presented as well as the conceptual design of its mechanics and electronics. Beam test results and measurements of irradiated LGAD silicon sensors, such as gain and timing resolution, will be shown.

**KEYWORDS:** Si microstrip and pad detectors; Timing detectors; Electronic detector readout concepts (solid-state); Performance of High Energy Physics Detectors

2018 JINST 13 C02016

---

## Contents

<b>1</b>	<b>Motivation</b>	<b>1</b>
<b>2</b>	<b>Detector requirements</b>	<b>1</b>
<b>3</b>	<b>Design and assembly — module components</b>	<b>2</b>
<b>4</b>	<b>Sensors and readout electronics</b>	<b>3</b>
<b>5</b>	<b>Prototypes testing</b>	<b>4</b>
5.1	HGTD test beam results for non irradiated sensors	4
5.2	Sensor performance after irradiation	5
<b>6</b>	<b>Conclusion</b>	<b>6</b>

---

## 1 Motivation

The high-luminosity phase of the Large Hadron Collider (HL-LHC) at CERN is foreseen to start in 2026 and deliver an integrated luminosity of  $4000 \text{ fb}^{-1}$  in about 10 years [1]. Pileup is one of the main challenges at the HL-LHC. In the nominal collision scheme, the interaction region will be spread over about 50 mm RMS along the beam axis, producing up to an average of 1.6 collisions/mm for an average pileup of 200 simultaneous  $pp$  interactions,  $\mu = 200$ . A powerful new way to address this challenge is to exploit the time spread of the interaction region to distinguish between tracks originating in collisions occurring very close in space but well-separated in time. This requires the ability to measure the time of tracks with a precision better than the time spread of the HL-LHC interaction region. In this context, a High-Granularity Timing Detector (HGTD) is proposed.

## 2 Detector requirements

HGTD will be located at about  $z = \pm 3.5$  m from the interaction region (figure 1), just outside the Inner Tracker subsystem (ITk) volume and in front of the endcap and forward calorimeters. It will cover the pseudorapidity region from about 2.4 to 4. Main parameters are presented in table 1. The exact number of layers (2 to 4) will be optimized according to the best compromise between performance and costs. The target is to achieve a time resolution of 30 ps per track. At the end of the HL-LHC, the maximum neutron-equivalent fluence at a radius of 120 mm ( $\eta=4$ ) should reach  $9 \times 10^{15} \text{ n}_{\text{eq}}/\text{cm}^2$  (including a safety factor). Consequently,  $4.5 \times 10^{15} \text{ n}_{\text{eq}}/\text{cm}^2$  and 4.5 MGy are the maximum expected doses in the sensors and ASICs, suggesting a replacement of the innermost part of the detector after half of the HL-LHC program.



**Figure 1.** A photo of the current ATLAS layout (opened for maintenance), showing the gap between the ATLAS endcap calorimeter on the left and the tracking detectors on the right, where the HGTD will be installed. Currently the space is occupied by the MBTS (white disk, in front of the endcap calorimeter).

**Table 1.** Main parameters of the HGTD.

Pseudorapidity coverage	$2.4 <  \eta  < 4.0$
Position in $z$	$3420 <  z  < 3545$ mm including 50 mm of moderator
Position of active layers	$3435 <  z  < 3485$ mm
Radial extension (active area)	110-1100 mm (120 - 640 mm)
Time resolution	30 ps per track

### 3 Design and assembly — module components

The HGTD detector concept is based on individual planar layers of LGAD sensors [2] to be fixed in front of both endcap calorimeter cryostats with active elements between 3435 and 3485 mm in  $|z|$ . On both sides of this cooling plate, individual identical modules consisting of LGAD sensors, ASIC and flex cables will be installed. The size of a module is  $2 \times 4$  cm $^2$  corresponding to a single LGAD sensor with two ASICs of  $2 \times 2$  cm $^2$  each bump-bonded on it. Figure 2 (left) shows three modules with the different components stacked in the  $z$  direction. First the ASICs will need to be bump-bonded to the LGAD sensor. This element will then be glued with accurate positioning on the flex cable used to transfer the signals. ASIC signals and HV connections will be performed by wire bonding to the flex cables. On the top and bottom sides of the cooling plate, the position of the modules is in a staggered arrangement. This configuration ensures a 20% overlap between modules. The modules disposition and stave orientation are still under optimisation. The modules located at a radius lower than approximately 300 mm are to be replaced after half of the HL-LHC program, due to the radiation damage in the sensors and ASICs. An intermediate thin plate will be used to pre-assemble and glue the modules and later screw in the cooling plate to allow a fast dismantling of the inner ring in a long shutdown and re-mounting of new modules. This concept is presented in figure 2 (right) where the green zone is the metallic plate at a radius lower than 300 mm. Yellow and blue squares represent the modules, orange and brown squares represent the flex cables.

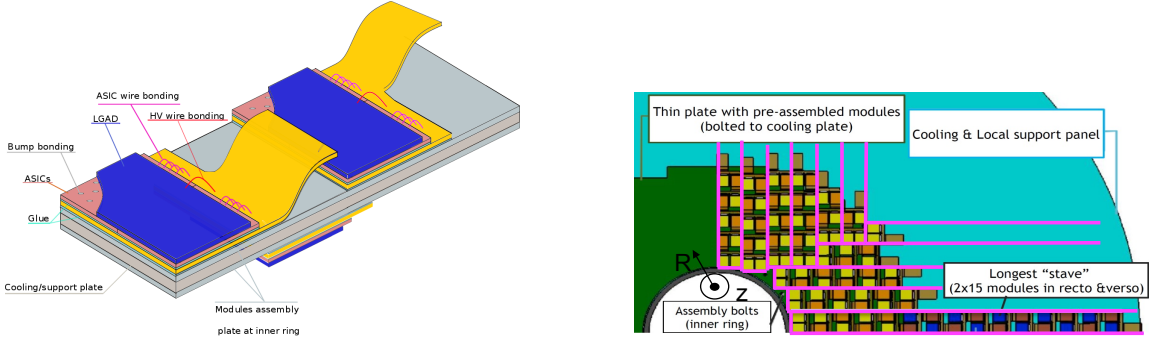


**Figure 2.** Schematic views showing two adjacent modules on the top side and one on the bottom side of the cooling plate and their assembly in one cooling plate.

#### 4 Sensors and readout electronics

The time resolution for the HGTD is required to be 30 ps per track over its full lifetime. The sensor pad size is restricted by occupancy, pad capacitance and the fill factor. A unified pad size of  $1.3 \times 1.3 \text{ mm}^2$  everywhere with an expected capacitance of 3.4 pF is found to fulfill the requirements. The pads will be arranged in arrays of total area of  $2 \times 4 \text{ cm}^2$  with a common backplane bias voltage connection. LGADs are planar silicon detectors with internal gain. Figure 3 shows one single pad sensor produced at CNM. They are n-on-p silicon detectors containing an extra highly-doped p-layer below the n-p junction to create a high field which causes internal gain as displayed in figure 3.

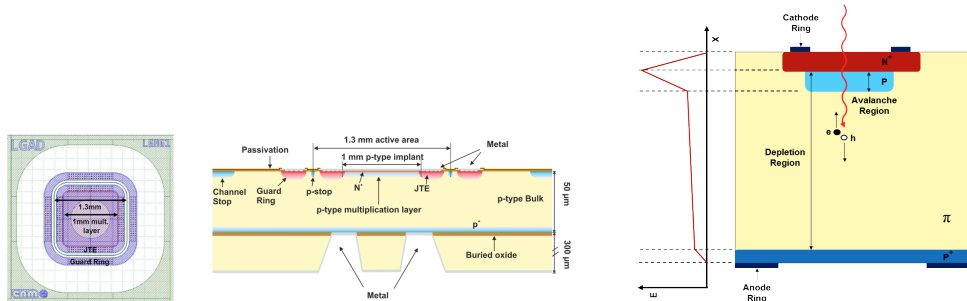


**Figure 3.** One single pad LGAD sensor produced at CNM and working principle of LGAD sensor.

The sensors will be read out by dedicated on-detector front-end electronics ASICs (bump-bonded to the sensors) which should keep the intrinsic excellent time resolution of the LGAD. The contribution to the time resolution from the electronics is given by:

$$\sigma_{\text{elec}}^2 = \sigma_{\text{jitter}}^2 + \sigma_{\text{Time Walk}}^2 + \sigma_{\text{TDC}}^2 \quad (4.1)$$

where  $\sigma_{\text{jitter}}$  depends on the noise and the pulse slope. The requirements of the ASIC, driven by the targeted 30 ps time resolution per MIP after irradiation by combining the multi-hits information, are summarized in table 2.

Each pixel readout channel will consist in a preamplifier followed by a discriminator, both defining elements for the overall electronics time performance (figure 4). A first prototype of the

**Table 2.** Front-end ASIC requirements, assuming that the sensors and ASICs in the inner region ( $R \leq 300$  mm) are replaced after half of the HL-LHC program.

Detector capacitance	3.4 pF
Number of channels/ASIC	225
Collected charge (1 MIP) at gain=20	9.2 fC
Dynamic range	1-20 MIPs
Total power per area (ASIC)	<200 mW/cm <sup>2</sup> (<800 mW)

ASIC, ALTIROC0, has been designed using the TSMC 130 nm process implementing both the preamplifier, the TOT and a CFD. The prototype chip contains eight channels, four optimized for a  $C_d$  of 2 pF and four optimized for larger capacitance. Measurements have been performed only on the 2 pF channels using a picosecond generator to provide a voltage test pulse with a rise time smaller than 100 ps. At 10 fC, a jitter of about 25 ps is measured.

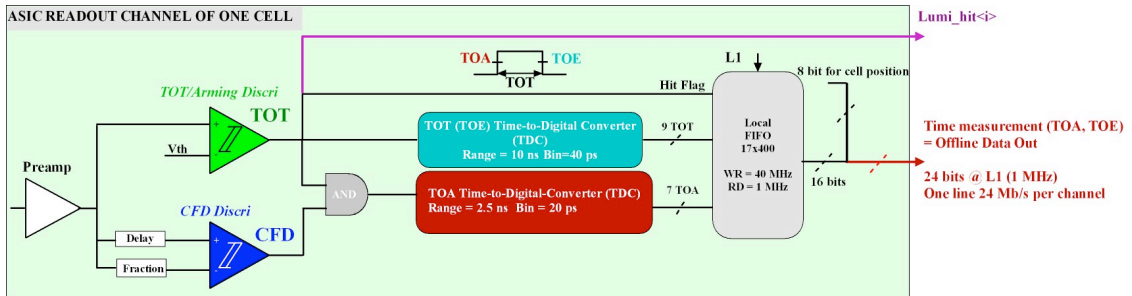


**Figure 4.** Schematic of a single pixel readout.

## 5 Prototypes testing

### 5.1 HGTD test beam results for non irradiated sensors

During beam tests in 2016 at CERN with 120 GeV pions [3], the gain was measured as a function of the position in the pads by combining the information from the beam telescope with the signal on the LGAD detector (see figure 5). The circular structure in the central part of the single pad sensor has a slightly lower gain than the external part.

The efficiency is defined at a given position in the pad as the number of hits that induce a sensor response (with amplitude above threshold) divided by the total number of reconstructed tracks crossing the sensor at that position. The measured 2D distribution for one single-pad sensor is shown in figure 6 (right). The time resolution has been studied in various beam tests. It has been consistently shown that sub-30 ps time resolution can be achieved below the breakdown point before irradiation for the  $1.3 \times 1.3$  mm<sup>2</sup> LGA devices with about 4 pF capacitance for all gain splits. Measurements based on data from the Autumn 2016 HGTD beam test show a best performance obtained for the ZCD algorithms. Figure 6 (right) presents the time resolution as a function of the gain for single pads and arrays. The best performance is obtained for the sensor with medium doping.

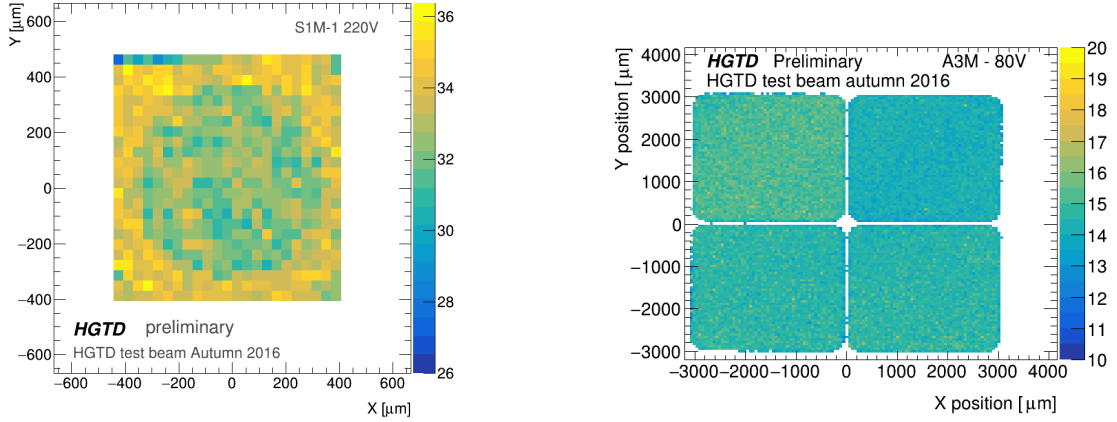


**Figure 5.** Gain for the single pad sensor as a function of the position in the pad with a bias voltage of 220 V (left) and gain for the array sensors as a function of the position on the sensor (right).

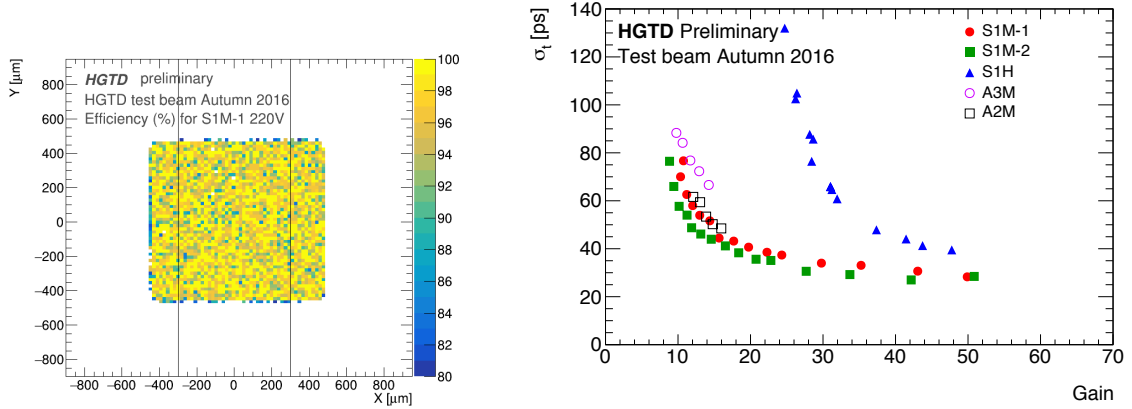


**Figure 6.** Efficiency in percent for the single-pad sensor, as a function of the position on the pad (left) and time resolution using the ZCD method as a function of the gain for single pad sensors and arrays (right).

## 5.2 Sensor performance after irradiation

The gain was found to decrease with irradiation which was attributed to loss of the effective doping concentration in the multiplication layer [4]. This can be observed in figure 7 (left) for CNM devices. The gain steadily decreases with irradiation and after fluences of  $6 \times 10^{14} \text{ n}_{\text{eq}}/\text{cm}^2$ . There is little difference between standard PIN and LGAD devices. Nevertheless gains of  $G=8$  were measured for devices irradiated to  $4 \times 10^{15} \text{ n}_{\text{eq}}/\text{cm}^2$ . The gain increases at lower temperatures due to an increase of impact ionization, whereas the breakdown voltage slightly decreases.

The timing performance of CNM LGADs irradiated to different fluences up to  $2 \times 10^{15} \text{ n}_{\text{eq}}/\text{cm}^2$  is shown in figure 7 (right). For HPK LGADs, the time resolution was measured with a  $^{90}\text{Sr}$  setup using the time difference to a calibrated thin LGAD. These results show that the currently available LGAD sensors can be operated safely up to a fluence of  $4.5 \times 10^{15} \text{ n}_{\text{eq}}/\text{cm}^2$ , keeping a time resolution of 50 ps, below the required limit of 60 ps per layer, in case of a 4 layers /side layout.

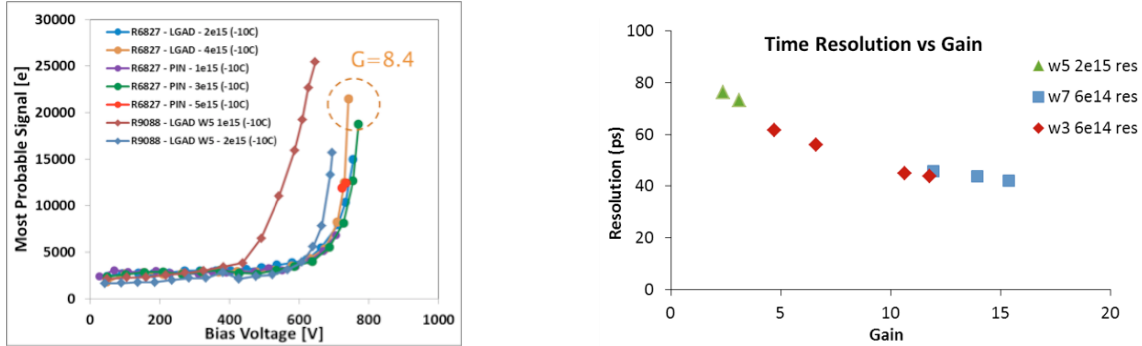


**Figure 7.** Most probable charge (or gain) dependence on bias voltage measured with  $^{90}\text{Sr}$  beta particles (Left) and Time resolution of neutron irradiated and non-irradiated CNM LGAD (right).

## 6 Conclusion

Requirements and design of a High-Granularity Timing Detector (HGTD), to be installed in ATLAS during the shutdown, (end of 2023–mid-2026) have been shown. First prototypes tests in beam tests and in the laboratory have been presented. This is the result of two years of active R&D, especially on sensors and front-end electronics by ~21 institutes and ~120 collaborators, started in summer 2015. The HGTD should provide a timing resolution of  $\sim 30$  ps for minimum-ionizing particles, covering the pseudorapidity region between 2.4 and 4.0. Intense R&D is ongoing with thinner sensors and different doping materials to increase even further the radiation resistance of the sensors.

## References

- [1] ATLAS collaboration, *ATLAS Phase-II upgrade scoping document*, [CERN-LHCC-2015-020](https://cds.cern.ch/record/2050200), CERN, Geneva Switzerland, (2015) [LHCC-G-166].
- [2] G. Pellegrini et al., *Technology developments and first measurements of Low Gain Avalanche Detectors (LGAD) for high energy physics applications*, *Nucl. Instrum. Meth. A* **765** (2014) 12.
- [3] L. Masetti et al., *Beam test measurements of Low Gain Avalanche Detector single pads and arrays*, publication in preparation, (2017).
- [4] J. Lange et al., *Gain and time resolution of 45  $\mu\text{m}$  thin Low Gain Avalanche Detectors before and after irradiation up to a fluence of  $10^{15} \text{ n}_{\text{eq}}/\text{cm}^2$* , *2017 JINST* **12** P05003 [[arXiv:1703.09004](https://arxiv.org/abs/1703.09004)].